

TRANSIENT CAVITATING PIPE FLOW: COMPUTATION MODELS AND METHODS

KAMIL URBANOWICZ AND ZBIGNIEW ZARZYCKI

*Department of Mechanical Engineering,
Szczecin University of Technology,
Al. Piastów 19, 70-310 Szczecin, Poland
{kurbanowicz, zbigniew.zarzycki}@ps.pl*

(Received 28 May 2008; revised manuscript received 3 July 2008)

Abstract: The paper presents four key mathematical models of a transient cavitating pipe flow, *i.e.* the column separation model (CSM), the gas cavitation model (CSMG), Adamkowski's model (CSMA) and the bubbly cavitation model (BCM). All models investigated in the paper take into account unsteady frictional loss models. The equations describing all models have been solved using the method of characteristics at first and the finite differences method then. The results of numerical simulations have been compared with the results obtained in the experiments. Transients which have taken into account the unsteady wall shear stress fit well with the results of experiments in comparison with the quasi-steady wall shear stress model.

Keywords: cavitation, transient turbulent pipe flow, unsteady friction, column separation, bubbly flow, numerical simulation

1. Introduction

A cavitation flow often occurs in an unsteady liquid flow in the pressure conduits of hydraulic and power machines and devices. Cavitation areas are observed in places where the pressure falls down to a value close to that of the liquid evaporation pressure at a given temperature. Their decay is accompanied by sudden pressure changes (which often occur cyclically). Under such conditions the flow is of a diphasic and quickly changing nature. In the literature on the subject there is no confirmed data on the character of cavitation areas, *i.e.* there is no information whether these areas are local or if they take place along the axis of a conduit.

Consequently, various models of transient cavitation calculation and simulation methods of an unsteady liquid flow in closed conduits with cavitation are used. The simplest calculation algorithm developed by Streeter [1] in 1969 which is based on the so-called column separation model (CSM) is applied in most of the computer software used for simulating an unsteady flow with cavitation.

The CSM model has had, in time, many modified versions, two of which should be mentioned: the vapor-gas cavitation model [2, 3] (CSMG) and Adamkowski's model [4] (CSMA). The former additionally takes into consideration the influence of

gas-cavitation on the waterhammer effect course whereas the latter makes it possible to carry discontinuities calculated in many cross-sections over to just one cross-section, while satisfying the mass and velocity conservation law at the same time.

A bubbly cavitation model (BCM) should be particularly noted [5, 6] among continuous cavitation models. It should be stressed that the above mentioned models take into consideration quasi-steady hydraulic resistance. By contrast, the present study takes into account friction losses which result from an unsteady flow. This approach makes it possible to take into account the unsteady wall sheer stress at wall in the equation of motion expressed by a convolution of liquid acceleration and a weighting function dependent on the flow's character (laminar or turbulent flow). The viscosity in this dependence (for the BCM model) is a function of liquid phase concentration of liquid and vapor viscosity.

Computer simulations of the waterhammer effect with cavitation for the four above mentioned models (CSM, CSMG, CSMA and BCM) were conducted taking into consideration both quasi-steady and unsteady friction losses. The simulation results were compared with the results of experiments. It was found that the results obtained through using models which took into consideration unsteady friction had a very good consistency with the experimental results.

2. Column separation models (CSM) – discreet models

Column separation models (CSM) are described by two equations [1, 2, 6] (which compose a closed system of quasi-linear differential equations and hyperbolic molecular equations with variable functions $v(x,t)$, $p(x,t)$) characterized by a one-dimensional unsteady liquid flow in pressure conduits and by boundary and initial conditions:

- continuity equation:

$$\frac{\partial p}{\partial t} + v \frac{\partial p}{\partial x} + c^2 \rho \frac{\partial v}{\partial x} = 0, \quad (1)$$

- momentum equation:

$$\frac{\partial v}{\partial t} + v \frac{\partial v}{\partial x} + \frac{1}{\rho} \frac{\partial p}{\partial x} + g \sin \gamma + \frac{2}{\rho R} \tau = 0, \quad (2)$$

where p – pressure, t – time, v – instantaneous mean flow velocity, x – distance along pipe axis, c – acoustic wave speed, ρ – liquid density (constant), g – acceleration due to gravity, γ – pipe slope angle, R – radius of pipe, τ – wall shear stress.

This kind of a system of equations is usually solved using the method of characteristics MOC [1, 2, 6]. Final equations make it possible to determine the flow parameters at internal nodes of the grid of characteristics (Figure 1).

The values of functions $v(x,t)$ and $p(x,t)$ depend on the specific devices installed at the inlet and outlet of a hydraulic, water supply or heating systems.

2.1. Vapor cavitation model

A traditional one-dimensional model of column separation (CSM) is the simplest discrete model which can be found in many papers on the subject [1, 2, 5–7].

When the pressure at an investigated node falls below the saturated vapor pressure, it is assumed that a cavitation area has appeared (Figure 2). It is also

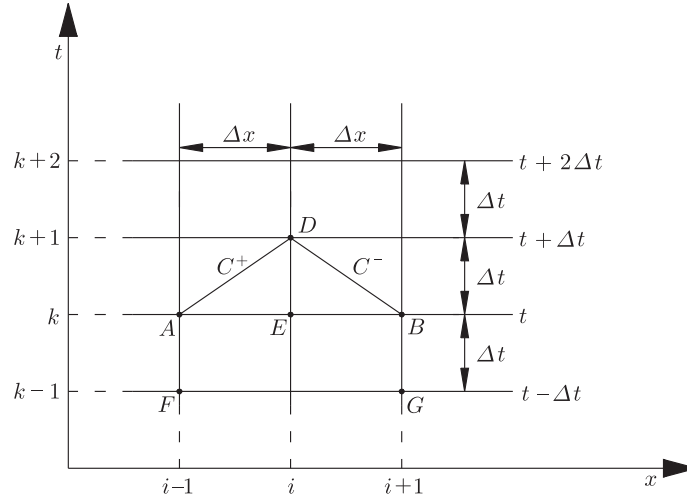


Figure 1. A grid of characteristics used for numerical calculations

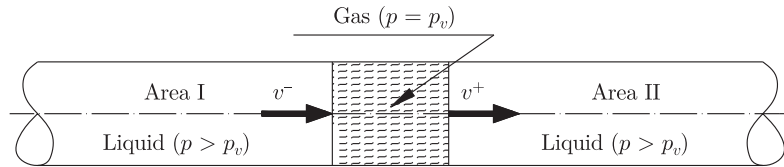


Figure 2. Flow with cavitation column separation

assumed that the pressure both inside and at the boundaries of the area is constant and that it is equal to the saturated vapor pressure $p_D = p_v$.

At the next step the velocity at both sides of a cavitation area (v_D^- – on the left side of separation and v_D^+ – on the right side of separation) is determined (Figure 3):

$$v_D^- = v_A + \frac{1}{c\rho} [p_A - p_v] - \frac{2\Delta t}{R\rho} \tau_A - g \sin \gamma \Delta t, \tag{3}$$

$$v_D^+ = v_B + \frac{1}{c\rho} [p_v - p_B] - \frac{2\Delta t}{R\rho} \tau_B - g \sin \gamma \Delta t, \tag{4}$$

where v_D^- is the liquid velocity from the inflow side (at the grid mesh), v_D^+ is the liquid velocity from the outflow side (at the grid mesh).

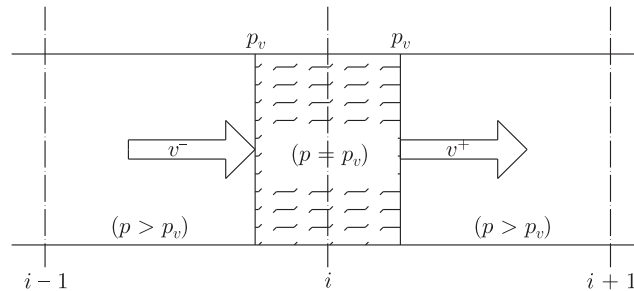


Figure 3. Velocity at the inlet and outlet of a discrete vapor area

An average flow value is determined in the intermediate cross-sections of the investigated pressure conduit. This approach is consistent with that of Safwat and Polder [8] who have assumed that the discontinuity area is formed in only one computational cross-section (which is the cross-section at the shut-off valve in this paper):

$$v_D = \frac{(v_D^+ + v_D^-)}{2}. \quad (5)$$

The cavitation area volume V_C in successive computational cross-sections is calculated from the following formula:

$$V_{C(k+1)} = V_{C(k)} + (\psi(v_{k+1}^+ - v_{k+1}^-) + (1 - \psi)(v_k^+ - v_k^-)) A \cdot \Delta t, \quad (6)$$

where ψ is the weight coefficient which in most studies [1, 2, 5–7] is assumed to be equal to 0.5, A – pipe cross-section area.

An assumption is made in this model that cavitation does not take place when $p_D > p_v$ and when $V_C \leq 0$.

When no cavitation occurs, the following equation is assumed: $v_D^- = v_D^+ = v_D$.

2.2. Adamkowski's model

In his in-depth analysis of a vapor cavitation model Adamkowski [4] has noticed artificial damping of pressure pulsation connected with column separation, despite the assumption that there are no hydraulic losses. In his opinion the damping is due to the fact that the model does not satisfy the conditions resulting from the principle of mass conservation and the momentum law. In his analysis, Adamkowski has also proved that the average flow velocity in sections where column separation has taken place should be determined from the following formula:

$$v = \text{sign} \left[(v_+ |v_+| + v_- |v_-|) + g \frac{V_C}{A} \sin \gamma \right] \sqrt{\left| 0.5(v_+ |v_+| + v_- |v_-|) - 0.5g \frac{V_C}{A} \sin \gamma \right|}, \quad (7)$$

where γ – pipe slope angle, V_c – cavitation zone volume (6).

2.3. Gas-vapor cavitation model

In [2, 3] Streeter and Wylie have presented the so-called separated air and vapor cavitation model which is a special case of a discrete model. The model proposed by Streeter and Wylie is based on the main equations which describe the waterhammer effect (1) and (2). In the continuity Equation (1) the pressure wave velocity in a diphasic mixture has been introduced in place of the pressure wave propagation velocity in water c :

$$c_m = c_l \cdot \left(\sqrt{1 + \frac{R_g \cdot T \cdot K_l \cdot m}{1 + \frac{K_l \cdot D}{E \cdot e}} \cdot \frac{m}{p^2}} \right)^{-1}, \quad (8)$$

where R_g is the universal gas constant, T is the absolute temperature [K], K_l is the liquid compressibility module, e – the conduit wall thickness, m – mass of free gas per unit volume of mix, E – Young's modulus, D – internal pipe diameter.

Next the system of Equations (1) and (2) has been solved using the method of characteristics which makes it possible to calculate both the desired functions $v(x, t)$ and $p(x, t)$ on the plane (x, t) and the cavitation area volume of column separation V_C with Equation (6).

Because the final equations take into account the changeable propagation velocity of a pressure wave (which depends on pressure), the numerical computational procedure which functions on a rectangular grid of characteristics must be based on interpolation and auxiliary iterative procedures. The authors of the model (of hydraulic transient) have noticed it themselves that the whole procedure is significantly complicated by interpolation and that it often leads to a false simulation [2]. Therefore, a few years after presenting a basic version of the model, its author, Wylie [3] has proposed to concentrate the precipitated gas in discrete areas of discontinuity and that the propagation velocity of a pressure wave between them should be treated as a constant equal to the velocity in liquid. A detailed description of how this particular model can be used can be found in a paper by Liou [9]. The paper suggests that in all the analysed cross-sections, when the pressure falls below the value of saturating liquid with a dissolved gas (usually with air), there appear some areas of discontinuity which are filled with gas. Additionally, when the pressure falls below the saturated vapor pressure, these areas expand to incorporate the areas which appear as a result of liquid evaporation.

According to a procedure which makes it possible to determine the current pressure and the average flow velocity it is required that the following system of non-linear equations should be solved [9]:

$$v_D^+ = v_B + \frac{1}{c\rho} [p_D - p_B] - \frac{2\Delta t}{R\rho} \tau_B - g \sin \gamma \Delta t, \tag{9}$$

$$v_D^- = v_A + \frac{1}{c\rho} [p_A - p_D] - \frac{2\Delta t}{R\rho} \tau_A - g \sin \gamma \Delta t, \tag{10}$$

$$-\frac{p_0 \alpha_0 \Delta x}{(p_D - p_v)^2} \cdot \frac{p_D - p_E}{\Delta t} = \psi (v_D^+ - v_D^-) + (1 - \psi) \cdot (v_E^+ - v_E^-), \tag{11}$$

where p_0 is the reference pressure, α_0 is the share of the gaseous area at pressure p_0 , ψ is the weight coefficient (for $\psi < 0.5$ the solution is not stable, for $\psi = 0.5$ the solution is stable, but it contains oscillations, and when $\psi > 0.5$ the solution is dumped [3]).

In this paper, it has been assumed that the weight coefficient $\psi = 0.6$ for this model during numerical simulations.

3. Bubbly cavitation model (BCM) – a continuous model

Despite the fact that the column separation model (CSM) can be easily used and that it truly reflects the nature of the problems and that it shows a high consistency with the presented physical phenomenon, it still has some serious disadvantages which have made Shu [5] develop an alternative model.

A diphase homogeneous equilibrium model of vapor cavitation is an alternative mathematical expression.

Differences between the velocity of liquid and gaseous (vapor) phases lead to a mutual exchange of momentum. However, these processes often take place very fast and it can be assumed that an equilibrium state dominates, *i.e.* vapor bubbles have the same velocity and pressure as the liquid. A bubbly cavitation model (BCM) has been developed on the basis of the last assumption.

The basic system of equations of an unsteady liquid flow with cavitation (continuity and momentum equations) for this model has the following form [5]:

$$\begin{cases} \frac{1}{c^2} \cdot \frac{\partial p}{\partial t} + (\rho_l - \rho_v) \cdot \frac{\partial \alpha}{\partial t} + \rho_m \cdot \frac{\partial}{\partial x} \cdot \left(\frac{v}{\alpha} \right) = 0, \\ \rho_m \cdot \frac{\partial}{\partial t} \cdot \left(\frac{v}{\alpha} \right) + \frac{\partial p}{\partial x} + \frac{2}{R} \tau \left(\frac{v}{\alpha}, \alpha \right) + \rho_m \cdot g \cdot \sin \gamma = 0, \end{cases} \quad (12)$$

where α – volumetric fraction of liquid, ρ_l – liquid density (constant), ρ_v – vapor density (constant), ρ_m – mixture density:

$$\rho_m = \alpha \cdot \rho_l + (1 - \alpha) \cdot \rho_v. \quad (13)$$

The second term in the continuity equation describes the value of interfacial mass penetration, whereas the component v/α reveals differences between the liquid phase flow velocity and the vapor phase flow velocity both in the continuity equation and in the amount of movement equation.

The above system of equations has been solved using the method of characteristics MOC [1, 2, 5, 6] (Figure 1).

4. The shear stress at a pipe wall

Any modeling of frictional resistance in transient flows should take into consideration unsteady flows. In the literature on the subject there are many quasi-steady hydraulic resistances [2, 3, 9]. It means that the shear stress at the wall of a pipe is determined according to Darcy-Weisbach's formula for the instantaneous average flow velocity. Currently, many recently published studies suggest that an instantaneous shear stress at the wall of a pipe τ can be given as a sum of a quasi-steady value τ_q and a variable which is changeable in time τ_n [5–7, 10, 11]:

$$\tau = \tau_q + \tau_n. \quad (14)$$

The value of τ_q is determined using a modified Darcy-Weisbach's formula [2]:

$$\tau_q = \frac{1}{8} \lambda \rho v |v|, \quad (15)$$

where λ – Darcy-Weisbach friction factor.

In a diphasic homogeneous non-slide flow, the above formula can be presented in the following form [5]:

$$\tau_q = \frac{\lambda \rho_m v |v|}{8 \alpha^2}. \quad (16)$$

The variable which is changeable in time τ_n can be determined from the following relationship [10–12]:

$$\tau_n = \frac{2 \cdot \mu}{R} \cdot \int_0^t w(t-u) \cdot \frac{\partial v}{\partial t}(u) \cdot du \quad (17)$$

where μ – dynamic viscosity coefficient, u – time at the convolution, $w(t)$ – weighting function.

The above relation describes the influence of an unsteady flow on the shear stress. This is the so-called convolution of an instantaneous liquid acceleration and a certain weight function. As can also be seen, the shear stress at the wall of a conduit

is a function of both velocity and time. The most precise form of the traditional weight function for a laminar flow has been presented by Zielke [12]:

$$w(\hat{t}) = \sum_{i=1}^6 m_i \hat{t}^{(i-2)/2}, \text{ for } \hat{t} \leq 0.02, \tag{18}$$

$$w(\hat{t}) = \sum_{i=1}^5 e^{-n_i \hat{t}}, \text{ for } \hat{t} > 0.02, \tag{19}$$

where $\hat{t} = \nu \cdot t / R^2$ is a dimensionless time and where coefficients m_i and n_i have the following values: $m_i = 0.28209, -1.25, 1.05778, 0.93750, 0.396696, -0.351563$; $n_i = -26.3744, -70.8493, -135.0198, -218.9216, -322.5544$.

There are two known traditional weight functions for a turbulent flow:

- that of Vardy-Brown [13]:

$$w(\hat{t}, \text{Re}) = \frac{A^* e^{-B^* \hat{t}}}{\sqrt{\hat{t}}}, \tag{20}$$

where $A^* = \sqrt{1/4\pi}$ and $B^* = \text{Re}^\kappa / 12.86$; $\kappa = \log_{10}(15.29/\text{Re}^{0.0567})$;

- and that of Zarzycki [10]:

$$w(\hat{t}, \text{Re}) = C \cdot \frac{1}{\sqrt{\hat{t}}} \cdot \text{Re}^n, \tag{21}$$

where $C = 0.299635$; $n = -0.005535$.

Unfortunately, the functions presented in these forms cannot be used in effective numerical methods whose aim is to seek a solution of the convolution (17).

The analyses conducted by many authors [11, 14–19] assume that only a weight function given as a finite sum of exponential expressions can be used in effective calculations.

A new, effective weight function is going to be used in this paper whose functionality has been significantly extended in comparison with the weight functions best known in the world. Additionally, the new weight function can be used both for unsteady laminar and turbulent flows.

The details about the origin of this function will be described in another paper.

A combination of laminar and turbulent functions has been possible owing to a scaling method presented by Vitkovsky *et al.* [17]. The function takes the form of Zielke’s function for a laminar flow (when $\text{Re} \leq 2320$), and its shape is modified using the scaling method for a turbulent flow (when $\text{Re} > 2320$). The coefficients used for scaling are identical to those used in traditional Vardy-Brown scales [13]. Owing to that the new scale adjusts its shape, given changes in the current Reynolds number (which characterizes unsteady flow), to the shape of Vardy-Brown scales.

The new effective laminar-turbulent scales used in this paper can be expressed as:

$$w_{\text{apr}}(\hat{t}) = \sum_{i=1}^{26} m_i e^{-n_i \hat{t}}, \tag{22}$$

where $m_1 = 1$; $m_2 = 1$; $m_3 = 1$; $m_4 = 1$; $m_5 = 1$; $m_6 = 2.141$; $m_7 = 4.544$; $m_8 = 7.566$; $m_9 = 11.299$; $m_{10} = 16.531$; $m_{11} = 24.794$; $m_{12} = 36.229$; $m_{13} = 52.576$; $m_{14} = 78.150$;

$m_{15} = 113.873$; $m_{16} = 165.353$; $m_{17} = 247.915$; $m_{18} = 369.561$; $m_{19} = 546.456$; $m_{20} = 818.871$; $m_{21} = 1209.771$; $m_{22} = 1770.756$; $m_{23} = 2651.257$; $m_{24} = 3968.686$; $m_{25} = 5789.566$; $m_{26} = 8949.468$; $n_1 = 26.3744$; $n_2 = 70.8493$; $n_3 = 135.0198$; $n_4 = 218.9216$; $n_5 = 322.5544$; $n_6 = 499.148$; $n_7 = 1072.543$; $n_8 = 2663.013$; $n_9 = 6566.001$; $n_{10} = 15410.459$; $n_{11} = 35414.779$; $n_{12} = 80188.189$; $n_{13} = 177078.960$; $n_{14} = 388697.936$; $n_{15} = 850530.325$; $n_{16} = 1835847.582$; $n_{17} = 3977177.832$; $n_{18} = 8721494.927$; $n_{19} = 19120835.527$; $n_{20} = 42098544.558$; $n_{21} = 92940512.285$; $n_{22} = 203458923.000$; $n_{23} = 445270063.893$; $n_{24} = 985067938.878$; $n_{25} = 2166385706.058$; $n_{26} = 4766167206.672$.

The universal values of coefficients are determined from the following formula:

$$\begin{aligned} n_{1u} &= n_1 - B^*; & n_{2u} &= n_2 - B^*; & \dots; & n_{26u} &= n_{26} - B^*, \\ m_{1u} &= m_1/A^*; & m_{2u} &= m_2/A^*; & \dots; & m_{26u} &= m_{26}/A^*, \end{aligned}$$

where, in turn:

$$A^* = \sqrt{\frac{1}{4\pi}}; \quad B^* = \frac{\text{Re}^\kappa}{12.86} = \frac{2320^\kappa}{12.86}; \quad \kappa = \log_{10}(15.29/\text{Re}^{0.0567}) = \log_{10}(15.29/2320^{0.0567}).$$

The universal values of the laminar-turbulent weight function coefficients which are based on scaling with Vardy-Brown coefficients are necessary to determine a current form of the weight function in a numerical process. The current values of coefficients which describe the weight function are determined on the basis of the above determined universal coefficients according to the following scheme (Figure 4).

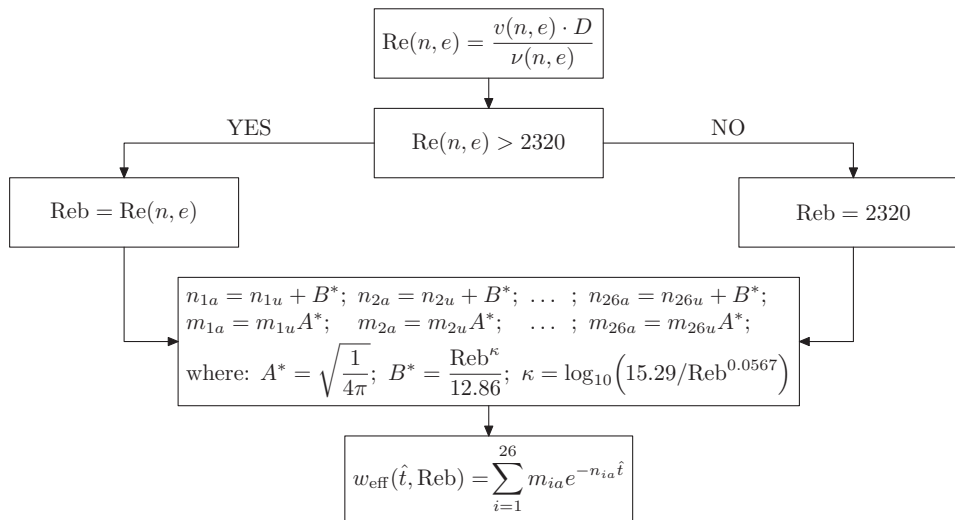


Figure 4. A scheme of the weight function selection

The above presented weight function has the following range of application: $0 \leq \text{Re} \leq 10^7$ and $10^{-9} \leq \hat{t} \leq \infty$.

5. Simulation studies and their comparison with the results of experimental studies

In order to assess which model best simulates an unsteady flow with cavitation, computer simulations were performed. Their results were compared with the results

of experimental studies conducted within the framework of the research project No. N504 029 31/2026 by A. Adamkowski and M. Lewandowski at a test station used for waterhammer effect studies at the PAS Institute of Fluid-Flow Machines in Gdansk (Figure 5). The main component of the test station is a pressure conduit made of copper $L = 98.56$ m in length, $D = 0.016$ m in inside diameter and $e = 0.001$ m in wall thickness. The conduit is spirally reeled on a steel roll with a diameter of approximately 1.7 m and it is stiffly mounted thereon in order to minimize vibrations excited by the waterhammer effect. The conduit's angle of inclination α is not larger than 0.5° . A ball valve with a quick shutoff action was installed next to a low pressure tank (the valve makes it possible to shut off the flow suddenly, almost instantaneously and fully). The speed of a complete shutoff was investigated and the shutoff time never exceeded 0.003 s which amounted to 1% of the propagation period of a pressure wave in this conduit ($4L/c$).

Five absolute pressure sensors (composed of semiconductor transducers) were mounted along the investigated conduit. The sensors' transfer band frequency was 0.2 kHz, their precision – 0.2% and their measuring range – 0–4 Mpa, which means that it was possible to record pressure changes in a time step of 0.0005 s (1/2000 Hz) which amounts to 0.17% of the propagation period of a pressure wave ($4L/a \approx 0.3$ s). The average flow velocity measurements were conducted with a turbine flowmeter whose range of application was $1.5 \text{ m}^3/\text{h}$ ($4.2 \cdot 10^{-4} \text{ m}^3/\text{s}$) and its precision was 1%.

The experimental system had been vented before the studies were commenced.

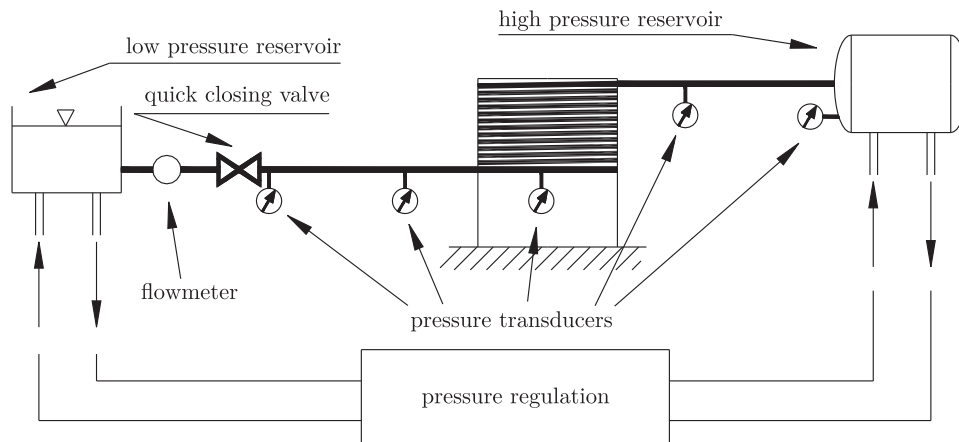


Figure 5. Test stand layout

5.1. Additional parameters of the system

Wave pressure propagation velocity: $c = 1280 \text{ m/s}$

Working liquid: water

Working liquid temperature : 22.6°C

Liquid density: $\rho = 1000 \text{ kg/m}^3$

Water vapor density : $\rho_p = 0.8 \text{ kg/m}^3$

Liquid kinematic viscosity: $\nu_c = 9.493 \cdot 10^{-7} \text{ m}^2/\text{s}$

Water vapor viscosity: $\nu_p = 8.7 \cdot 10^{-9} \text{ m}^2/\text{s}$

Initial flow velocity – run I: $v_0 = 1.9$ m/s

Initial flow velocity – run II: $v_0 = 2.76$ m/s

Pressure at the pressurized reservoir – run I: $p_t = 406$ kPa

Pressure at the pressurized reservoir – run II: $p_t = 682$ kPa

5.2. Quantitative analysis

Valuation of maximum pressure values and times of its occurrence in the analyzed transient flow is very important from the point of view of operational specificity. No mathematical quantitative methods useful for comparison of simulated runs with reference to experimental runs are shown in the available articles concerning a transient flow with cavitation. All authors have focused only on a qualitative estimate.

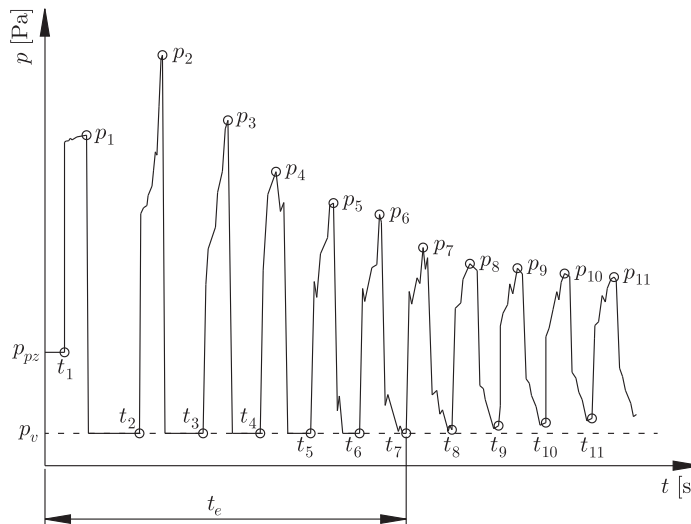


Figure 6. Transient pipe flow with cavitation

A quantitative analysis in this research work will rely on appointment of two parameters (p_p and t_p) characterizing the degree of adjustment to an experimental run. Values of maximum pressures (Figure 6 – p_1 to p_n) for all pressure amplitudes of the researched run make it possible to assign the following parameter p_{pi} :

$$p_{pi} = \frac{p_{si} - p_{ei}}{p_{ei}} \cdot 100\%, \quad (23)$$

where p_{ei} – value of the maximum pressure on the analyzed i amplitude, based on an analysis of experimental results; p_{si} – value of the maximum pressure on the analyzed i amplitude, based on an analysis of the simulated results.

The value of the above parameters p_{pi} , depends on the n value of the analyzed pressure amplitudes. Knowing all the above parameters for the analyzed runs it is possible to determine the following parameter:

$$p_p = \sum_{i=1}^n \frac{|p_{pi}|}{n}. \quad (24)$$

A similar analysis will be carried out for the time (Figure 1 – t_1 to t_n) of appearance of pressure amplitudes:

$$t_{pi} = \frac{t_{si} - t_{ei}}{t_{ei}} \cdot 100\%, \tag{25}$$

where t_{ei} – time of appearance of i amplitude of pressure, based on an analysis of experimental results; t_{si} – time of appearance of i amplitude of pressure, based on an analysis of simulated results.

When all t_{pi} values for the analyzed run are known, it is possible to describe the correspondence of the simulation with reference to the experimental run with the following parameters:

$$t_p = \sum_{i=1}^n \frac{|t_{pi}|}{n}. \tag{26}$$

When the values of p_p and t_p get lower, then it is better to adjust the simulated runs with reference to the experimental runs.

5.3. Results of simulations

A detailed quantitative and qualitative analysis will concern changes of pressure in a pipe cross section near the valve because it is where the result of hydraulic impact which take place in waterhammer case with cavitation will be strongest. Two runs

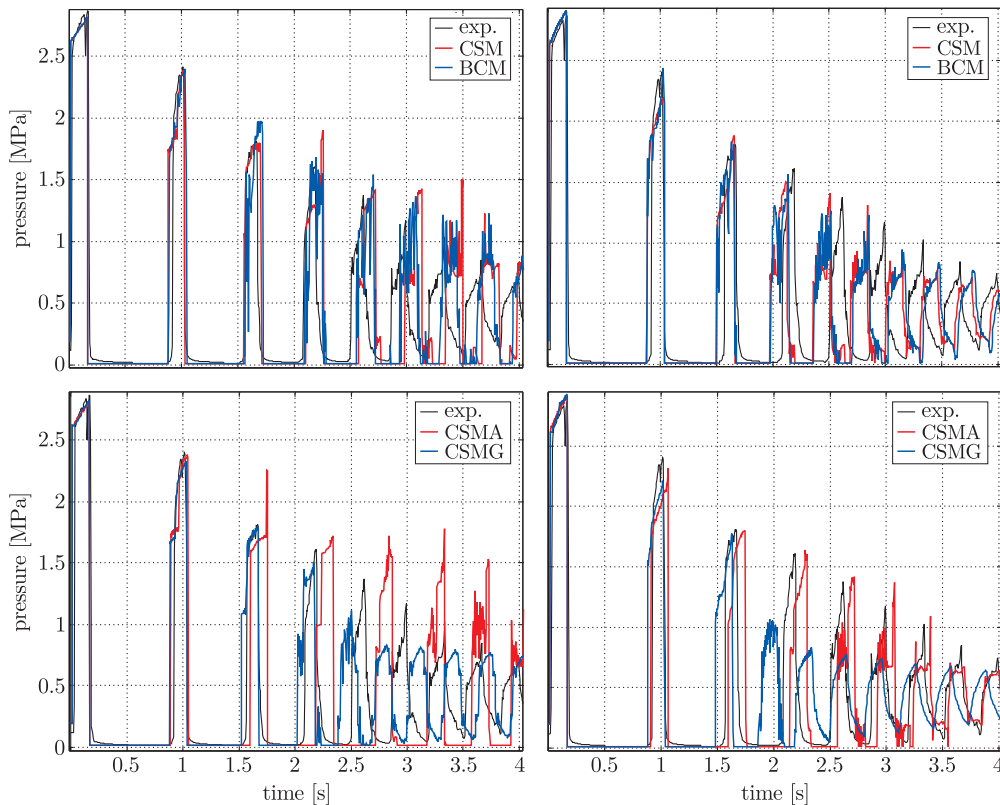


Figure 7. Pressure runs at the cross-section near the valve (run I: $v_0 = 1.9\text{m/s}$; left – quasi-steady resistance, right – unsteady resistance)

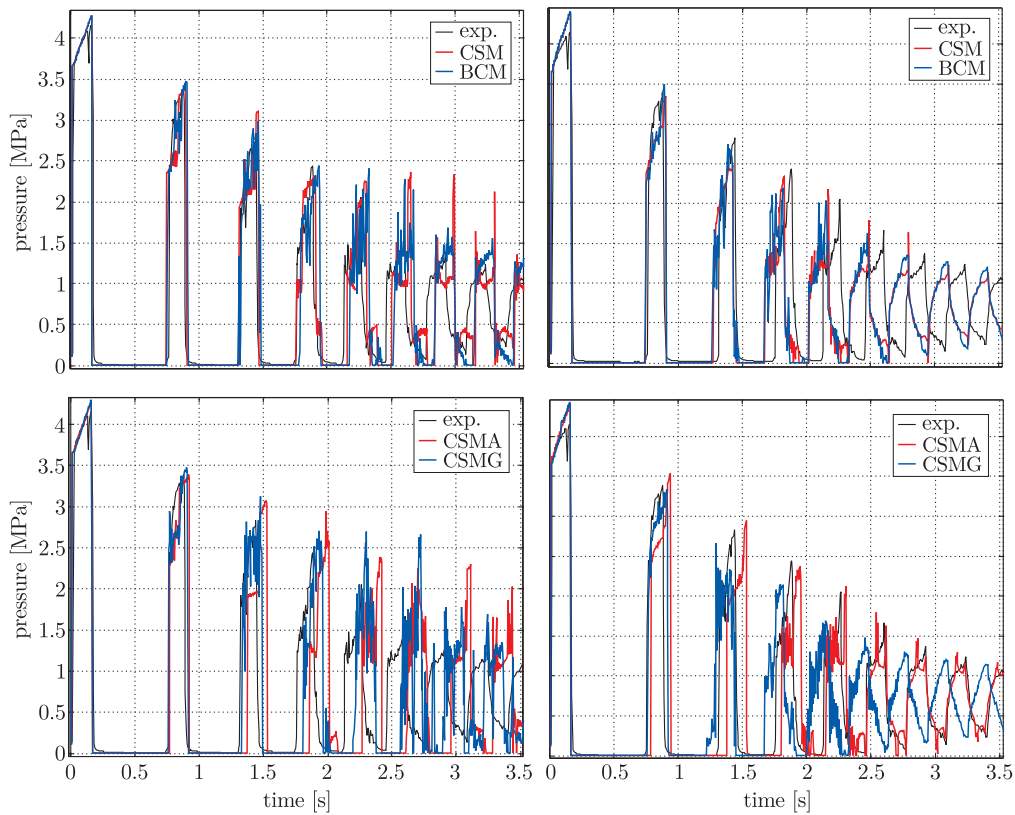


Figure 8. Pressure runs at the cross-section near the valve
(run II: $v_0 = 2.76$ m/s; left – quasi-steady resistance, right – unsteady resistance)

Table 1. Quantitative analysis – unsteady hydraulic resistance

parameter	CSM model	CSMA model	CSMG model	BCM model
p_p [%] (run I)	7.6243	6.4420	20.6780	3.5918
p_p [%] (run II)	6.2687	4.8740	9.1263	4.1309
t_p [%] (run I)	5.1134	1.8429	9.9296	4.8729
t_p [%] (run II)	3.6856	2.8320	5.1370	4.0735

Table 2. Quantitative analysis – quasi-steady hydraulic resistance

parameter	CSM model	CSMA model	CSMG model	BCM model
p_p [%] (run I)	17.0534	29.8039	10.9550	13.3190
p_p [%] (run II)	11.8069	13.7999	19.6891	10.9295
t_p [%] (run I)	3.2108	7.8393	4.6517	2.3111
t_p [%] (run II)	1.0113	4.9971	2.3227	1.4609

will be analyzed. The results of both simulation and experimental studies (pressure variations near the valve) are shown below.

Only new modified models which take into consideration unsteady hydraulic resistance will be considered in a qualitative analysis of the above examples of simulation studies. All the above presented graphs of models using the quasi-steady resistance (which can be seen on the left hand side in Figures 7 and 8) have been presented for comparison purposes only, to show to the reader of this present paper a significant difference between them and the models in which unsteady resistance has been taken into account (these models have been shown on the right hand side of Figures 7 and 8).

A detailed qualitative analysis of the obtained results (run I, run II and all other runs not shown in this work) showed that almost all the models of an unsteady flow with cavitation (which took into consideration unsteady hydraulic resistance) were quite good in simulating the investigated flow. It was only the vapor-gas cavitation model (CSMG) that was characterized by excessive dumping and consequently the results obtained while using the model had serious errors. Adamkowski's model (CSMA) was best at simulating the times of successive pressure amplitudes. Both CSM and BCM models were characterized by greater dumping than the CSMA model owing to which they simulated the appearance of successive amplitudes slightly earlier than in the experiment.

The results of the quantitative analysis are shown below in Table 1 and Table 2.

The first eight pressure amplitudes were analyzed in run I and only six in the next run (run II). The quantitative analysis shows that the BCM model has the best agreement in terms of simulating maximum pressures (it is not clearly visible in Figures 7 and 8). This analysis confirms also a conclusion from the qualitative analysis that Adamkowski's model is the best model for simulating the times of successive pressure amplitudes. Models in which unsteady hydraulic resistance is included have shown a definitely better degree of adjusting than models using quasi-steady resistance (see percentage results in Table 1 and Table 2).

6. Conclusions

Four models of an unsteady flow with cavitation have been presented at first and then compared in this paper. Three models, *i.e.* the so-called discrete models are based on the column separation theory. These include the traditional model of column separation (CSM), Adamkowski's model (CSMA) and the vapor-gas cavitation model (CSMG). The BCM model is continuous and, according to the cavitation areas, cavitation can take place at any section of a pressure conduit, not only at nodal sections.

The detailed conclusions drawn on the basis of all the above studies are as follows:

- the CSM, BCM and CSMA models which use a new, effective model of unsteady hydraulic resistance are very good at simulating unsteady states with cavitation. The best of all the three models is Adamkowski's model of column separation (CSMA) which correctly simulates both the time when successive pressure amplitudes appear and their respective maximum values;
- the vapor-gas cavitation model (CSMG) which takes into account unsteady hydraulic resistance is characterized with too intensive dumping and therefore

it cannot be commonly used. The model was developed at the time when unsteady hydraulic resistance was not taken into account and when scholars only considered their quasi-steady character. At that time the model provided the best consistency of all other models, which is evidenced by the earlier presented simulations (Figures 7 and 8 – the graphs on the left hand side).

- other discrepancies which can be seen between simulation and experimental runs are probably due to: changes of the average propagation velocity of a pressure wave which are caused by gas cavitation (during an unsteady flow with cavitation), the fact that convective derivatives were omitted, the assumption made for simplicity purposes that liquid movement had one-dimensional character, errors of numerical methods.

References

- [1] Streeter V L 1969 *ASCE, J. Hydraulic Division* **95** (6) 1959
- [2] Wylie E B and Streeter V L 1978 *Fluid Transients*, McGraw-Hill, New York
- [3] Wylie E B 1984 *J. Fluid Engng* **106** 307
- [4] Adamkowski A and Lewandowski M 2007 *Proc. FEDSM 2007, 5th Joint ASME/JSME Fluids Engineering Conference*, San Diego, California USA, CD-ROM
- [5] Shu J J 2003 *Int. J. Pressure Vessels and Piping* **80** 187
- [6] Urbanowicz K and Zarzycki Z 2007 *Trans. Institute of Fluid-Flow Machinery*, The Szwedzki Institute of Fluid-Flow Machinery, Gdansk, **120** 53
- [7] Zarzycki Z and Urbanowicz K 2006 *Chemical and Process Engineering*, PAS, Wrocław, **3/1, tom 27** 915 (in Polish)
- [8] Safwat H H and Polder Jaap van Den 1973 *J. Fluids Engng* **95** 91
- [9] Liou J C P 2000 *J. Fluids Engng* **122** (3) 636
- [10] Zarzycki Z 2000 *Proc. 8th Int. Conf. on Pressure Surges*, The Hague, The Netherlands, BHR Group Conference Series, **39**, pp. 529–534
- [11] Zarzycki Z and Kudźma S 2004 *Proc. 9th Int. Conf. on Pressure Surges*, Chester, UK, BHR Group, pp. 439–455
- [12] Zielke W 1968 *J. ASME* **90** 109
- [13] Vardy A E and Brown J M B 2003 *J. Sound and Vibration* **259** (5) 1011
- [14] Trikha A K 1975 *J. Fluids Eng., Trans. ASME* **97** 97
- [15] Schohl G A 1993 *J. Fluids Eng., Trans. ASME* **115** 420
- [16] Kagawa T, Lee I Y, Kitagawa A and Takenaka T 1983 *Trans. Japan Society of Mechanical Engineers Ser B* **49** (447) 2638 (in Japanese)
- [17] Vítkovský J P, Stephens M L, Bergant A, Simpson A R and Lambert M F 2004 *9th Int. Conf. on Pressure Surges*, Chester, United Kingdom, pp. 405–419
- [18] Kudźma S 2005 *Modeling and Simulation Dynamical Runs in Closed Conduits of Hydraulics Systems Using Unsteady Friction Model*, PhD Thesis, Szczecin University of Technology (in Polish)
- [19] Vardy A E and Brown J M B 2004 *J. Hydraulic Engng* **130** (11) 1097